Journal of Applied Fluid Mechanics, Vol. 17, No. 1, pp. 89-104, 2024.
Available online at www.jafmonline.net, ISSN 1735-3572, EISSN 1735-3645.
https://doi.org/10.47176/jafm.17.1.2126

Parametric Investigation of Pelton Turbine Injector under Hydro-abrasive Erosion Conditions

N. Shrivastava† and A. K. Rai

Department of Mechanical Engineering, National Institute of Technology Warangal, Warangal 506004, India

†*Corresponding Author Email: ns720040@student.nitw.ac.in*

ABSTRACT

In high-head Pelton turbines, the injector faces severe erosion due to suspended sediment leading to a reduction in turbine efficiency and higher maintenance costs. Here, the effects of design parameters such as the bend angle of the nozzle pipe, nozzle angle, and needle angle along with an operating parameter stroke ratio on hydro-abrasive erosion of Pelton turbine injector are numerically investigated. The Volume of Fluid (VOF) model was implemented for capturing the interphase between air and water; whereas, the SST k-ω model is used for modelling the turbulence effect. For tracking the discrete phase, a Eulerian-Lagrangian based Discrete Phase Model (DPM) is considered. The bend angles led to flow circulations in the nozzle pipe causing the non-uniform distribution of sediment concentration and uneven erosion patterns. Irrespective of the bend angle, the erosion hotspot in the needle is observed toward the bend side. Further, for larger sediment particles, higher bend angles lead to more erosion rate in both the nozzle and needle and must be avoided to prevent excessive damage. As the needle angle increases from 40° to 60° for a constant nozzle angle, the nozzle erosion rate increases by 70% and the needle erosion rate decreases by 99%. Hence, an injector design can be optimized in hydro-abrasive erosion conditions by selecting a needle angle between 40° and 60°. Further, the operation of the injector at too high and low a stroke ratio results in excessive erosion of the nozzle and needle, respectively. In this study, a stroke ratio of 0.45 is found to be the most suitable for hydro-abrasive erosion conditions. Moreover, the asymmetricity in the erosion pattern of the needle increases with needle angle and stroke ratio resulting in jet quality degradation, one major reason for efficiency reduction in Pelton turbines.

Article History

Received July 1, 2023
Revised August 30, 2023
Accepted September 12, 2023
Available online November 1, 2023

Keywords:

Hydropower
Hydro-abrasive erosion
Pelton injector
Bend angle
Nozzle and needle angle

1. INTRODUCTION

Among all renewable-based energy, hydropower contributes the most in power generation and accounts for around 53.7% of all renewable-based power produced worldwide in year 2021 (IEA, 2022). The suspended sediments present in the water restricts the power generation, especially in hydropower plants (HPP) situated in the geologically young mountain range of the Himalayas of South Asian region (Sangal et al., 2018; Shrivastava & Rai, 2023). About 59% of the total sediment entering the ocean comes from Asian rivers (Dedkov & Gusarov, 2006). Especially during monsoon and snow-melt seasons, a significant increase in sediment inflow in the streams leads to higher damages of the hydraulic turbine components from hydro-abrasive erosion in run-of-the-river HPPs; whereas, reduced storage capacity in reservoir based HPPs (Bajracharya et al., 2008; de Miranda & Mauad, 2015; Luis et al., 2016; Rai et al., 2017; Arora et al., 2022).

Hydro-abrasive erosion is a destructive process that alters the profile of hydraulic turbine components resulting in efficiency reduction and renewable energy generation loss (Padhy & Saini, 2012; Felix, 2017). For the Chilime Pelton turbine HPP, Bajracharya et al. (2008) estimated an efficiency loss of 1.21% for the first year and 4% for the successive year at the 3.4 mm/year of the erosion rate. For the Jhimruk Francis turbine HPP, efficiency loss of 4% and 8% were observed due to sediment erosion in two months of operation for full load and part load conditions, respectively (Thapa et al., 2015). Further, in addition to efficiency reduction, hydro-abrasive erosion results in the increase of maintenance and operating cost of an HPP (Rai et al., 2019). Though hydro-

NOMENCLATURE			
D_O	Nozzle exit diameter	V	Fluid velocity
d_r	Reference particle diameter	V_i	Impact velocity
H	Head of plant	V_p	Particle velocity
H_v	Vickers hardness of wall material	α	Impact angle
p	Pressure	μ	dynamic viscosity
$\dot{Q}$	Discharge	ρ	Fluid density
S	Stroke length	ρ_p	Particle density
U	Velocity vector	Ø	discharge coefficient

abrasive erosion is observed in all types of hydraulic turbines in sediment-laden flow, the Pelton turbines are the most affected due to high heads. The high head (800 m -1300 m) leads to high flow velocity in Pelton turbine components like injectors and buckets making even small particles with sizes less than 60 μm causing severe damage (Padhy & Saini, 2008, 2011).

The injector experiences the highest velocities and in turn, eroded extensively resulting in degraded jet quality. The quality of the jet depends on the injector design as well as operating condition and plays a significant role in the performance of a Pelton turbine (Zhang & Casey, 2007; Staubli et al., 2009a, 2010; Jung et al., 2019). The hydro-abrasive erosion in a Pelton injector depends on sediment parameters like size, size distribution, concentration, shape, and hardness; impact parameters like sediment impact velocity and impact angle; operating parameters like the head of an HPP and nozzle opening; design parameters like bend pipe angle, nozzle angle, needle angle, nozzle exit diameter, bucket width, the radius of the curved region of bucket and material of turbine components (Rai et al., 2020; Ge et al., 2021; Bajracharya et al., 2022; Tarodiya et al., 2022). Different empirical correlations relating hydro-abrasive erosion and efficiency with different parameters are obtained by the researchers, but they are confined to a specific range (Liu et al., 2019; Padhy & Saini, 2009; Rai et al., 2020). This is because hydro-abrasive erosion is a complex and progressive process and collecting continuous variable data during HPP operation is a laborious and challenging task (Rai & Kumar, 2015).

Erosion in the Pelton injector is mainly due to cutting action because of the lower angle of impact of sediment particles. From the field study at Chenani HPP, Din and Harmain (2020) observed crater formation a little upstream of the needle tip and nozzle exit due to a higher impact angle compared to the needle tip and upper region of the nozzle where ripple marks were formed. With the increase in sediment concentration, the erosion rate in the Pelton injector increases as more particles strike the surface. IEC 62634 (2019) gives the linear relation between hydro-abrasive erosion and sediment concentration, also observed by Rai et al. (2020) during the experimental study of the Pelton turbine. Specific regions of the needle and nozzle of a Pelton injector with the maximum flow velocity experience high erosion. For the needle, the erosion hotspot is a little upstream of its tip; whereas, it is at the exit for a nozzle (Messa et al., 2019; Guo et al., 2020). The Pelton needle is highly susceptible to wear during part load conditions compared to full load conditions due to the synergic effect of hydro-abrasive erosion and cavitation (Bajracharya et al., 2008; Din & Harmain, 2020). Moreover, during part load conditions, the number of sediment particles striking the needle surface increases as more particles reflecting from the nozzle surface rebound towards the needle surface (Bajracharya et al., 2021). Secondary flow and vortices formation take place in the Pelton injector due to pipe bend and needle guide resulting in an asymmetrical erosion pattern (Guo et al., 2020; Han et al., 2021). However, the effect of the inclination of a bend on the secondary flow and erosion pattern is not completely explored yet.

Hydro-abrasive erosion can be mitigated by using a desilting tank at the inlet of penstock; however, due to technical and economical limitations, constructing a desilting tank able to remove particles finer than 200 μm is not considered (Bajracharya et al., 2008; Koirala et al., 2016; Rai et al., 2016). Therefore, erosion mitigation requires other methods such as optimizing the design and flow condition and replacing target material with higher erosion-resistant material or by surface modification of base material (Messa et al., 2019; Singh & Nath, 2022; Tarodiya et al., 2022). Rai et al. (2020) tested the erosion behaviour of six different materials of Pelton bucket including softer material brass as well as 13Cr-4Ni martensitic stainless steel with WC-Co-Cr HVOF coating. Due to high susceptibility to hydro-abrasive erosion, soft materials like brass are not used in manufacturing high head Pelton turbines; whereas, WC-Co-Cr HVOF coated martensitic stainless steel is the most preferred material to mitigate hydro-abrasive erosion. Tarodiya et al. (2022) observed coated Pelton injector with WC-Co-Cr coated martensitic stainless-steel resists 100 times more than an uncoated one. Further, they observed erosion resistance of high-velocity air fuel (HVAF) processed WC-Co-Cr to be higher than high-velocity oxy-fuel (HVOF) processed. Messa et al. (2019) and Tarodiya et al. (2022) effect of nozzle-needle on its hydro-abrasive erosion rate. However, the effect of bend angle on the severity of erosion still needs to be explored. Further, the effects of sediment size on the erosion pattern of an injector with a bend nozzle pipe are not considered in the earlier studies. Tarodiya et al. (2022) compare the erosion rate of the Pelton injector for a different combination of the nozzle-needle angle in pair. However, the effect of a specific design parameter i.e., nozzle angle or needle angle has not been investigated yet.

In this study, the Pelton injector with external servomotor is taken by considering a high head of 820 m corresponding to the head of Kashang HPP for the simulation. Thereafter, the design parameter of the Pelton injector is optimized with respect to hydro-abrasive

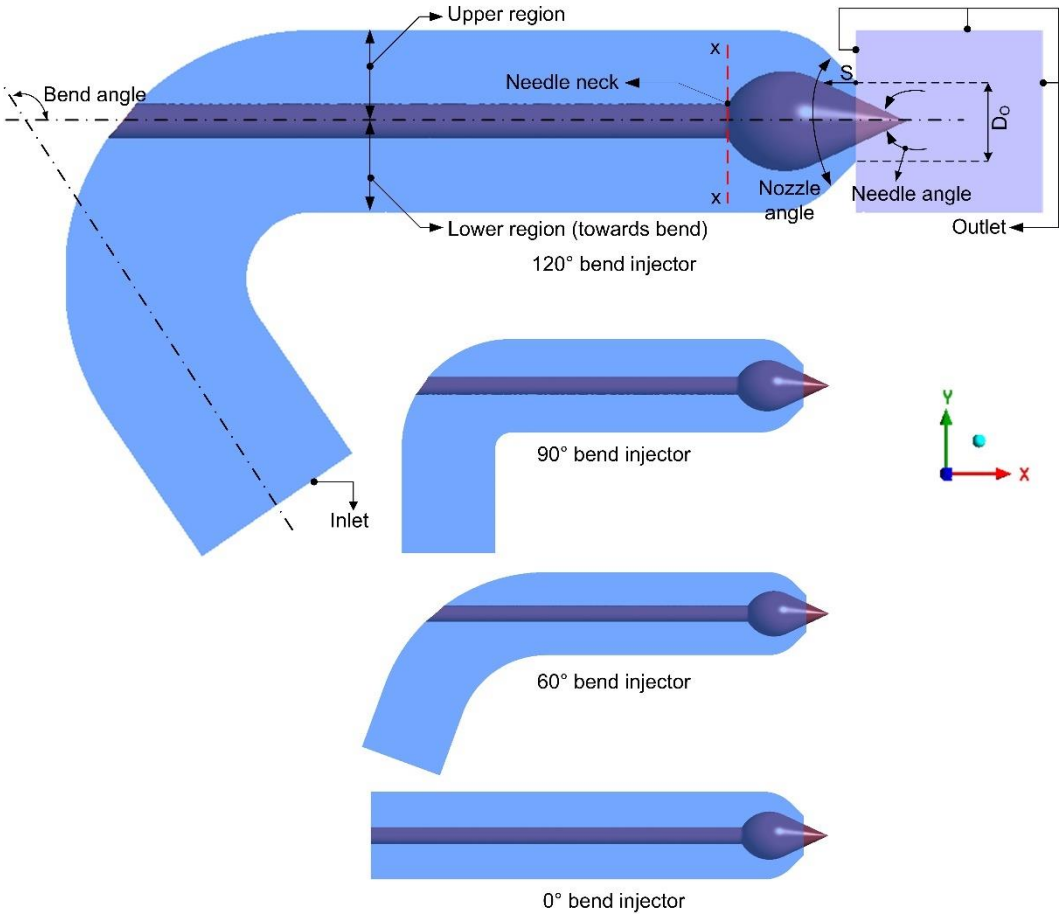

Fig. 1 Design and computational domain without needle guide vane considered for analysis

erosion. This paper consists of four sections. First is an introduction with having literature review of studies related to the hydro-abrasive erosion process in the Pelton turbine, second is the methodology, discussing geometrical and numerical modelling used in the study, third is the results and discussion section where obtained numerical results are described in detail and last is the conclusion, presenting the major findings observed while caring out this study.

2. METHODOLOGY

This section elaborates on the design and meshing details of the Pelton injector considered in this study along with the different numerical techniques implemented for obtaining hydro-abrasive erosion. Further, details of the validation of the numerical scheme are also provided.

2.1 Geometrical Model and Meshing

In this paper, the Pelton injector with external servomotor is considered for investigation and is designed using inlet Design Modeler software. To observe the effect of pipe bend angle on the erosion rate and pattern for two different sediment sizes (10 µm and 100 µm), various bends considered in the injector design are shown in Fig. 1. Other design parameters investigated include nozzle angle and needle angle variation. Further, the effect of loading on erosion is also observed by varying the stroke ratio which is a ratio of stroke length (S) and nozzle exit diameter (D_O) as shown in Fig. 1. For investigating various design cases, the exit diameter of the nozzle (D_O) is taken as 100 mm and the stroke ratio is considered constant as 0.45. Here, the x-x section at the exit of the needle rod is named as needle neck as shown in Fig. 1.

A structured mesh is generated using Ansys meshing software having minimum orthogonal quality and maximum skewness of 0.32 and 0.71, respectively. To capture the erosion and flow phenomenon, a dense meshing is used near the area of interest i.e., the nozzle exit region - erosion hotspot region and the needle tip region - boundary layer formation as shown in Fig. 2 (Guo et al., 2020). A mesh with 2.81 million elements is considered for simulation after carrying out a mesh independence test for saving the computational time since the mass flow rate barely varied after 2.81 million mesh elements as shown in Fig. 3.

2.2 Numerical Schemes and Mathematical Model

Pelton turbines situated at a high head experience severe erosion - one of such hydropower plants is Kashang HPP. Therefore, at the inlet, pressure equivalent to the head of the Kashang HPP was taken. At the outlet, zero-gauge pressure was selected while operating pressure of 1atm was considered. At inlet turbulence effect is included by giving values for turbulent intensity and hydraulic diameter as per Ansys Fluent User Guide manual assuming fully developed flow (Ansys Fluent User's Guide 15.0). The Kashang HPP, consists of 3 units of 5 jet Pelton turbines with 8.99 m^3/s unit discharge and a designed head of 820 m, with a total installed capacity of 195 MW (3 x 65 MW). The present study considers the inlet pressure equivalent to the high head of the Kashang

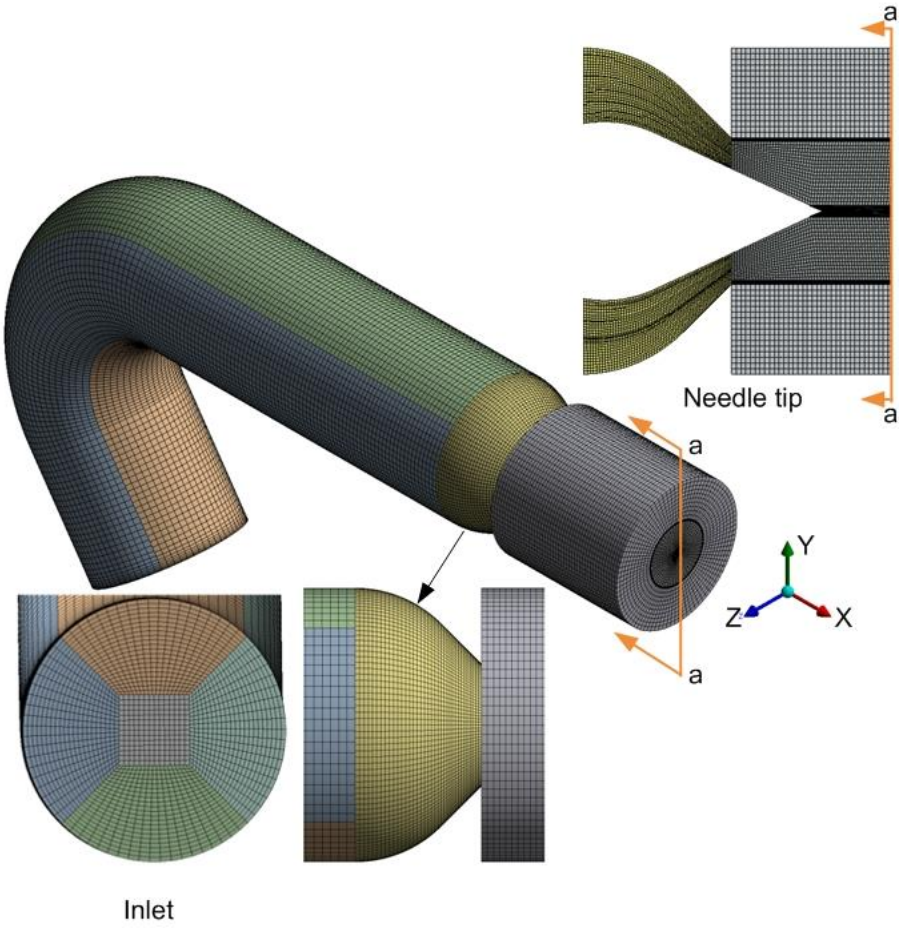

Fig. 2 Structured mesh of computational domain

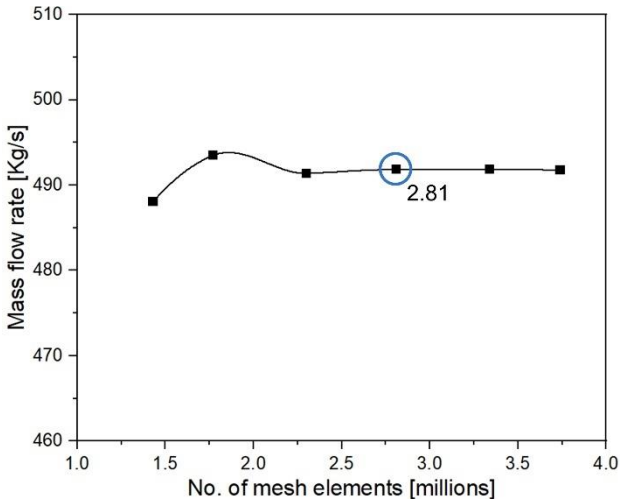

Fig. 3 Mesh independence test

HPP since limited CFD studies on injector considering head value greater than 500 m is available. In actual hydropower plants with high capacity 65 MW turbine, internal servomotor design is frequently used; however, the erosion behavior of such designs was already available in the literature (Messa et al., 2019; Guo et al., 2020). Thus, the present study considers the reference of Kashang HPP for qualitative validation of erosion patterns and selecting a high value of plant head i.e., 820 m for simulation. Accordingly, single bend is considered with simplification for simulation rather than an entire distributor. Moreover, simulating various design and operating parameters considering the entire distributor would have been computationally expensive. For capturing the interface between continuous phases of air and water, the Volume of Fluid (VOF) model was selected, and its continuity and momentum governing equation is given by equation (1) and equation (2) respectively. In the VOF model, the properties of the mixture (ɱ) depend on the volume fraction of the phases and are represented by equation (3) (Hirt & Nichols 1981).

$$\nabla\cdot(\rho U) = 0 \tag{1}$$

$$\nabla\cdot(\rho UU) = -\nabla p + \nabla\cdot[\mu(\nabla U + \nabla U^{T})] + \rho g \tag{2}$$

$$ɱ = ɱ_{a}\Phi_{a} + ɱ_{w}\Phi_{w} \tag{3}$$

In the above equation the symbols ρ, U, p, μ, and g represent mass density, velocity vector, pressure, dynamic viscosity, and acceleration due to gravity, respectively. Whereas $ɱ_{a}$, $ɱ_{w}$ represent general properties and Φ_{a}, Φ_{w} represent the volume fraction of air and water respectively.

For tracking the discrete phase i.e., sediment particles, Discrete Phase Model (DPM) is considered. In the DPM model, continuous and discrete phase is modelled using Eulerian and Lagrangian based approach, respectively. The governing equation depicting the DPM model is represented by equation (4).

$$\frac{dV_{p}}{dt} = F_{D}(V - V_{p}) + \frac{g(\rho_{p} - \rho)}{\rho_{p}} + F \tag{4}$$

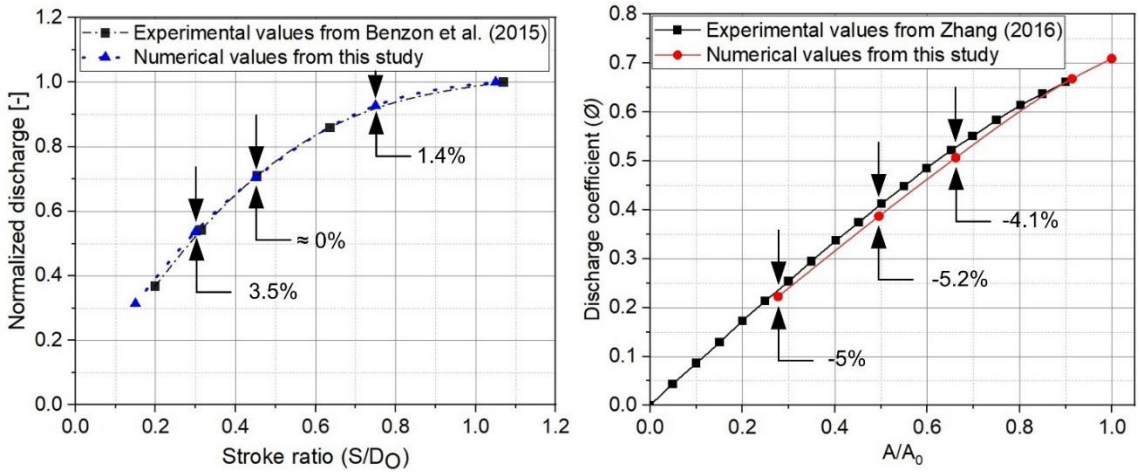

Fig. 4 Validation of obtained numerical result with experiment of (a) Benzon et al. (2015) and (b) Zhang (2016)

In the above equation, V, V_p, t, ρ_p and F represents fluid velocity, particle velocity, time, particle density, and additional force per unit mass, respectively; whereas $F_D(V-V_P)$ term represents the drag force per unit particle mass and the term F_D is given by equation (5).

$$F_D = \frac{18\mu C_D Re}{\rho_P d_P^2 24} \tag{5}$$

where, C_D, Re, and d_P are drag force coefficient, Reynolds number, and particle diameter, respectively. To calculate the drag coefficient, the Spherical Drag law is used assuming sediment particles to be smooth and spherical in shape as provided in equation (6).

$$C_D = a_1 + \frac{a_2}{Re} + \frac{a_3}{Re^2} \tag{6}$$

where, a_1, a_2, and a_3 are constants. The mass density of sediment particles is taken as 2650 kg/m^3 i.e., equal to the density of quartz which is present in abundance in sediment-laden water reaching HPP (Rai et al., 2017; Din & Harmain, 2020). As the density ratio i.e., the ratio of the mass density of water to sediment is greater than 0.1, therefore, additional forces constituting virtual mass and pressure gradient forces are also considered and are given by equation (7) and equation (8) respectively (Ansys Fluent Theory Guide 15.0).

$$F_V = \frac{1}{2}\frac{\rho}{\rho_P}\frac{d}{dt}(V - V_P) \tag{7}$$

$$F_P = \frac{\rho}{\rho_P} V_p \nabla V \tag{8}$$

where, F_V and F_P are virtual mass force and pressure gradient force per unit mass respectively. As the sediment concentration considered is 750 ppm which is much below 1% hence one-way coupling is selected in this study (Xu et al., 2016). The turbulence dispersion of the discrete phase was predicted using Random Walk Model (RMW), a stochastic method.

For the prediction of the erosion rate, an in-built Ansys Fluent Oka erosion model was selected and is given by equation (9) (Oka et al., 2005, Oka & Yoshida 2005). For modelling turbulence effect SST k-ω turbulence model was selected as it gives considerable results for both near and away from wall regions, giving benefits of both k-ω and k-ε turbulence model. Further, for simultaneously solving the continuity and momentum equation, and linking pressure and velocity Coupled algorithm was selected.

$$E = E_{90}\left(\frac{V_i}{V_r}\right)^{k_1}\left(\frac{d_P}{d_r}\right)^{k_2} f(\alpha) \tag{9}$$

where E_{90} is the reference erosion ratio at normal impact, V_i is the impact velocity of a particle, V_r is reference velocity, d_r is reference particle diameter, k_1, and k_2 are velocity exponent and diameter exponent respectively and $f(\alpha)$ is impact angle function and is given by equation (10).

$$f(\alpha) = (\sin\alpha)^{n_1}\left(1 + H_v(1 - \sin\alpha)\right)^{n_2} \tag{10}$$

where, α, H_v, n_1, and n_2 are impact angle, Vickers hardness (Gpa) of wall material, and angle function constants, respectively. To account for the loss in the momentum of sediment particles after rebounding from the injector wall, the Forder restitution model was considered and is represented by equation (11) and equation (12) (Forder et al., 1998).

$$\varepsilon_n = 0.988 - 0.78\alpha + 0.19\alpha^2 - 0.024\alpha^3 + 0.027\alpha^4 + 0.027\alpha^4 \tag{11}$$

$$\varepsilon_t = 1 - 0.78\alpha + 0.84\alpha^2 - 0.21\alpha^3 + 0.028\alpha^4 - 0.022\alpha^5 \tag{12}$$

where, ε_n and ε_t are coefficients of restitution in normal and tangential directions respectively and α is particle impact angle in radians.

2.3 Validation

The accuracy of the numerically obtained result was compared with the experimental work of Benzon et al. (2015) and Zhang (2016). In the first validation, the normalized discharge i.e., the ratio of maximum obtained discharge to local discharge is observed for different loading conditions i.e., stroke ratio, and the observed variation of numerically obtained normalized discharge closely resembles the experimental values obtained by Benzon et al. (2015) as shown in Fig. 4a. In the second

Fig. 5 Erosion contour obtained in this study and eroded needles of Kashang HPP having excessive erosion towards bend side of injector

Table 1 Sediment, design and operating parameters considered in the study

S. No.	Parameter fixed	Parameters considered
1	Nozzle angle: 90° Needle angle: 50° Stroke ratio: 0.45	i. Bend angle (0°, 60°, 90°,120°) for sediment size 10 µm ii. Bend angle (0°, 60°, 90°,120°) for sediment size 100 µm
2	Bend angle: 120° Nozzle angle: 90° Stroke ratio: 0.45	Needle angle (40°, 50°, 60°) for sediment size 100 µm
3	Bend angle: 120° Needle angle: 50° Stroke ratio: 0.45	Nozzle angle (80°, 90°, 100°) for sediment size 100 µm
4	Bend angle: 120° Nozzle angle: 90° Needle angle: 50°	Stroke ratio values (0.3, 0.45, 0.75, 1.05) for sediment size 100 µm
5	Bend angle: 120° Nozzle angle: 90° Needle angle: 50° Stroke ratio: 0.45	Needle guide vane orientation angle (0°, 45°, 90°) for sediment size 100 µm

validation, variation of discharge coefficient (Ø) given by equation (13) is plotted with respect to the ratio of the area of nozzle opening at local partial opening condition (A) to full opening condition (A_O). It was observed, the curve obtained from the numerical results of the current work is in good alignment with the values obtained from the experimental work of Zhang (2016) as shown in Fig. 4b. Further, a simulation is carried out considering Rossin - Rammler size distribution considering sediment size between 30 µm and 120 µm and obtained erosion pattern of needle is compared with eroded needle of Kashang HPP. Similar to needle of Kashang HPP, excessive erosion obtained numerically is observed towards the bend side of the needle as shown in Fig. 5. Table 1 shows various parameters considered while carrying out this study with all cases without needle guide vanes except S. No. 5.

$$Ø = \frac{4\dot{Q}}{\pi D_O^2 \sqrt{2gH}} \tag{13}$$

where $\dot{Q}$ and H are discharge and head of HPP respectively.

3. RESULTS AND DISCUSSION

In this section, the variations in erosion intensity and pattern observed for different design conditions that includes the bend angle of nozzle pipe, needle angle, and nozzle angle as well as the operating condition having different values of stroke ratio are discussed.

3.1 Effect of Bend Angle of Nozzle Pipe

Velocity streamlines are plotted at the needle neck section for different bend angles (0°, 60°, 90°, and 120°) as shown in Fig. 6. It is observed, for 0° bend all streamlines are straight having uniform velocity distribution whereas for an injector with a bend, streamline is curved with an increase in non-uniformity in velocity distribution as bend angle increases. The formation of Dean vortices having less velocity compared to other regions is observed at the lower side, such that the size of Dean vortices increases with the bend angle. In this paper region below the nozzle axis towards the bend side and the region above the nozzle axis is mentioned as the lower and upper region of the injector, respectively. Similar Dean vortices formation toward the bend side is also observed by Staubli et al. (2009b) shown in Fig. 6. For smaller size sediment with 10 µm size the intensity of erosion does not vary much though the erosion pattern does with increase in bend angle, as shown in Fig. 7. For both nozzle and needle erosion pattern is more uniform for 0° compared to the injector with a bend as shown in Fig. 7.

For larger sediment with 100 µm size, both erosion rate as well as pattern vary with the bend angle of the nozzle pipe. For the nozzle, erosion rate increases from a bend angle of 0° bend to 90°, but with a further increase in bend angle from 90° bend to 120° change in erosion rate

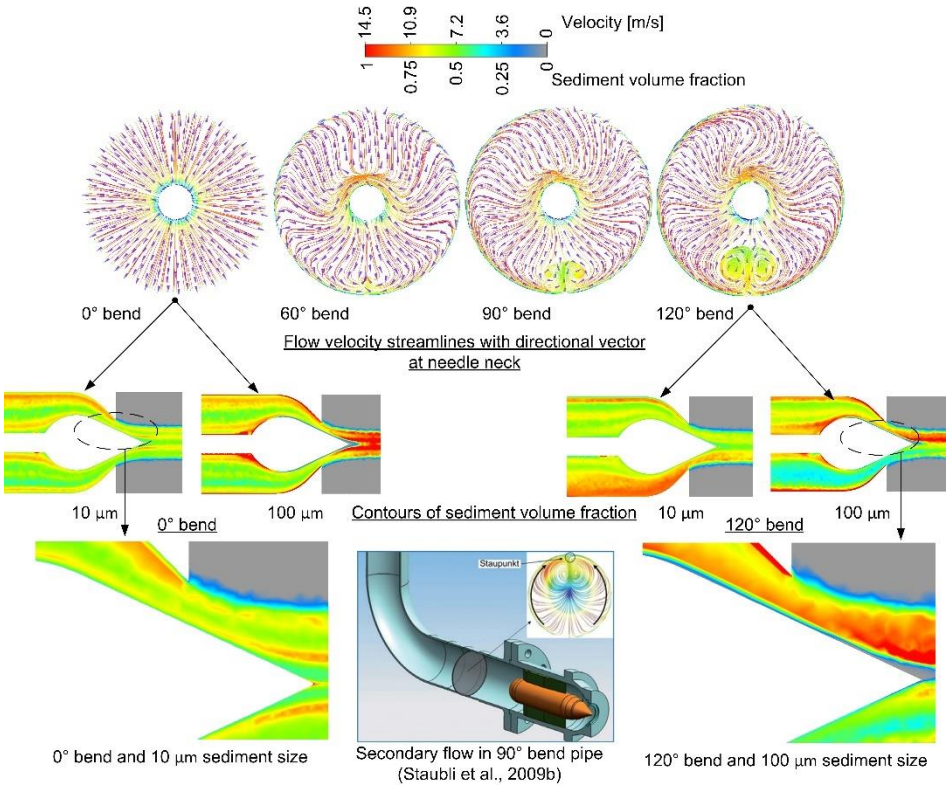

Fig. 6 Variation in velocity streamlines and sediment volume fraction in Pelton injector with bend angle of nozzle pipe

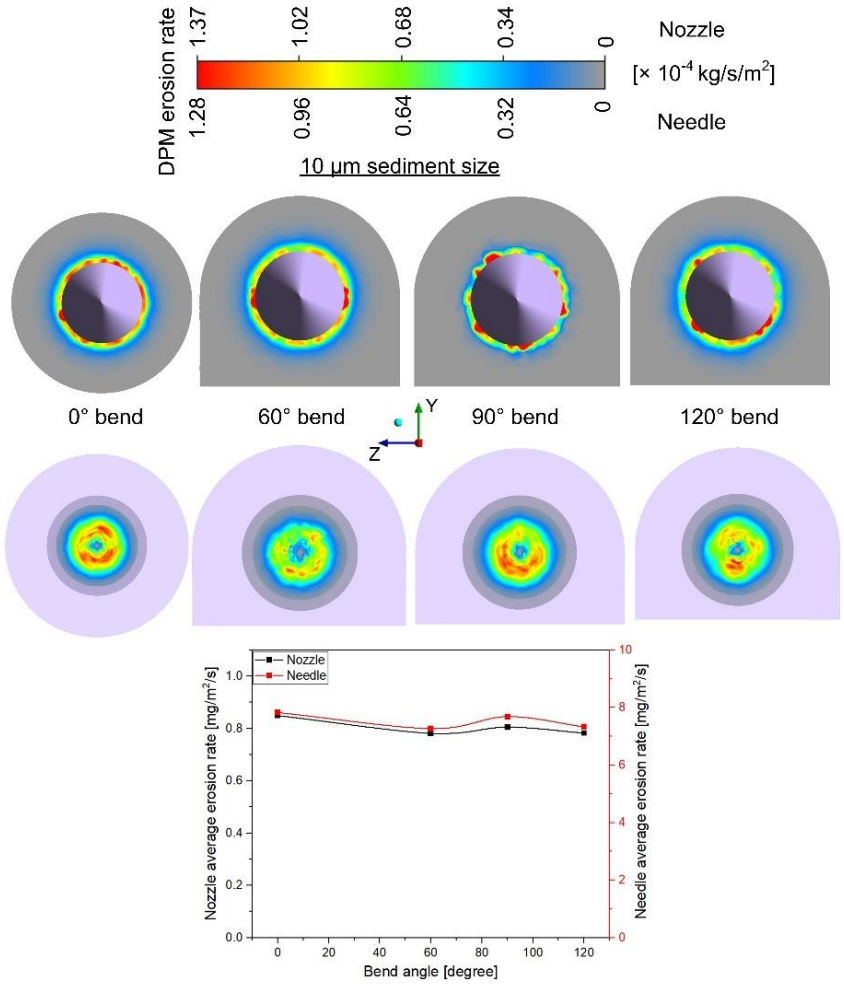

Fig. 7 Variation of erosion rate of nozzle and needle with nozzle pipe bend angle for 10 µm sediment size

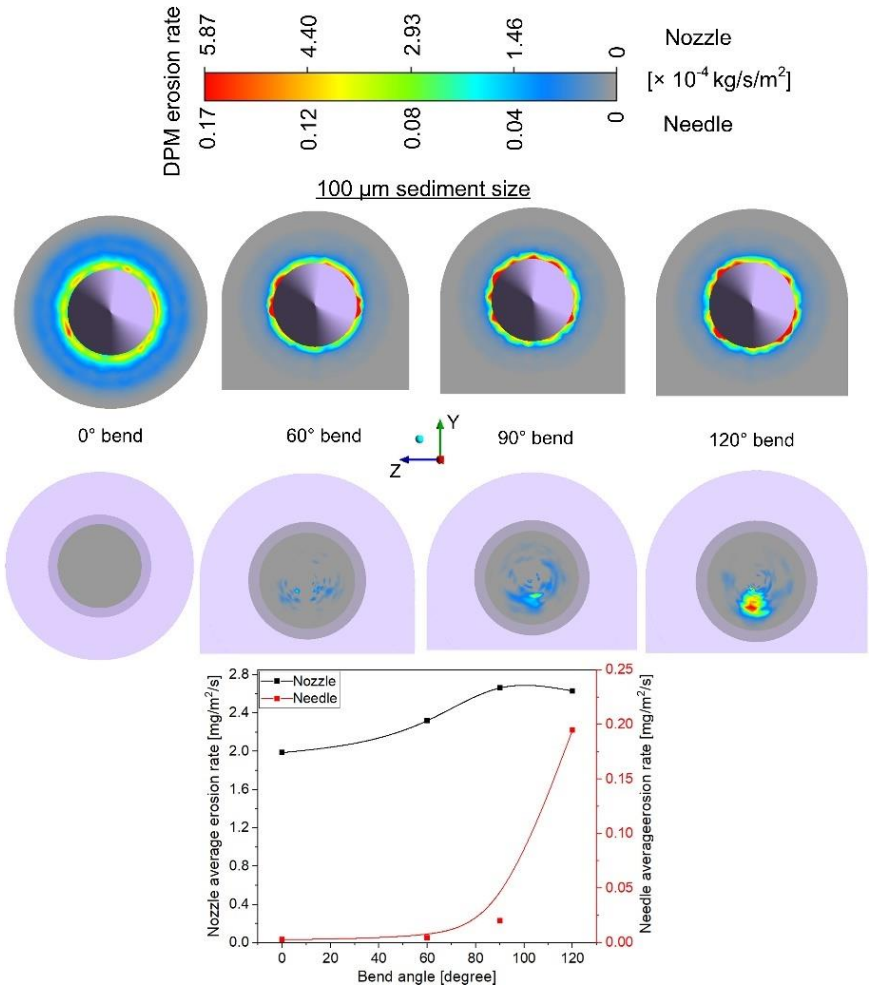

Fig. 8 Variation of erosion rate of nozzle and needle with nozzle pipe bend angle for 100 µm sediment size

is less notable as shown in Fig. 8. For, 60° intensity of the erosion is more in the upper region of nozzle however as bend angle increases from 60° to 120° erosion pattern becomes more uniform shown in Fig. 8. Due to the high inertia of 100 µm sediment particles, they are more likely to get separated from fluid flow as shown in Fig. 6. As a result, for 0° bend angle, sediment particles in larger quantity, distributed uniformly along the radial direction strikes the convergent region of the nozzle, having lesser velocity than the region at nozzle exit resulting in a reduction in erosion intensity as shown in Fig. 8. It is also observed, in nozzle erosion due to large particles is more severe than smaller particles due impact of sediment with higher kinetic energy is the former case.

In needle erosion caused by small sediment particles is more severe than caused by larger particles. This is due to the tendency of smaller particles to follow a fluid path more closely than larger particles. As shown in Fig. 6 small particles following the fluid path, strikes a high-velocity region, of the needle region i.e., a little upstream of the needle tip. Whereas, most of the large particles strike the low-velocity region i.e., the needle neck loses its momentum due to this sediment in very less concentration striking the region a little upstream to the needle tip, resulting in less erosion as shown in Fig. 6. Further, for larger particles erosion hotspot in needle of a bend injector is observed in the lower region. This is due to low velocity in the lower region compared to the upper region as a result lower region particles follow the fluid path more closely striking the needle surface at a higher concentration compared to the upper region as shown in Fig. 6. Further it is observed, with increase in bend angle needle erosion caused by larger particles increases, due to increase in low velocity region having vortices formation as shown in Fig. 6 and Fig. 8.

3.2 Effect of Needle Angle

While comparing the erosion rate of the Pelton injector with respect to the needle angle for a fixed nozzle angle, it is observed, that as the needle angle increases from 40° to 60° erosion rate of the nozzle also increases as shown in Fig. 9. This is because, as the needle angle increase, the needle becomes more bulge with a bigger maximum diameter. Due to this, sediment in high concentration is directed toward the nozzle exit region as shown in Fig. 10, increasing the nozzle erosion rate. For the needle abrupt increase in erosion rate is observed with a decrease in needle angle from 60° to 40° as shown in Fig. 9. This is because the surface of the needle exposed to higher flow velocity increases with a decrease in needle angle as shown in Fig. 10. This causes an increase in the number of particles having higher kinetic energy striking the needle surface, finally increasing needle erosion rate. Though the erosion hotspot in the needle is observed in the lower region but for the needle with 40° tip angle, erosion is observed in the upper region as well which eventually

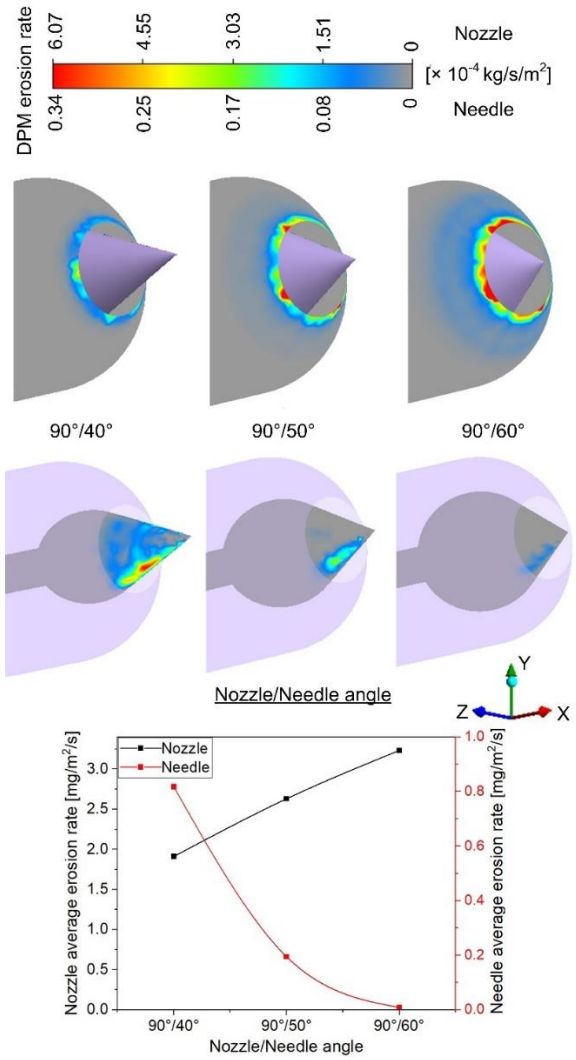

Fig. 9 Variation of erosion rate of nozzle and needle with needle angle

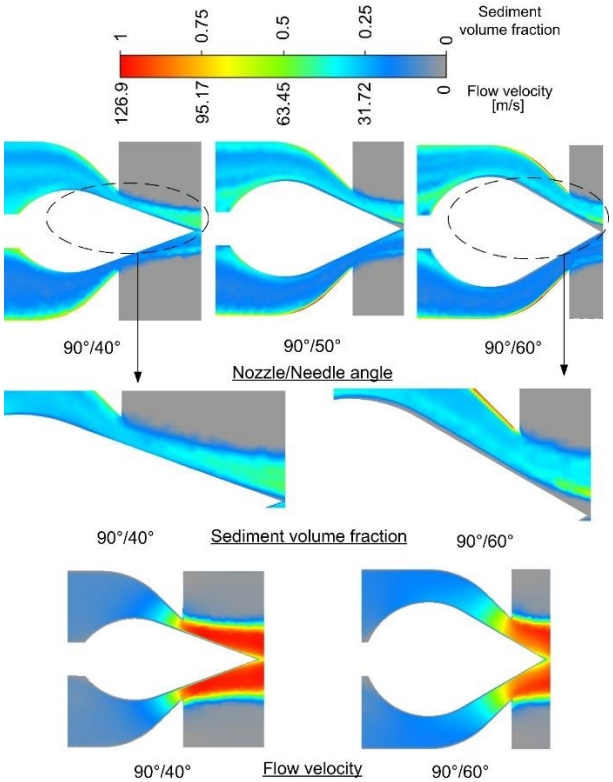

Fig. 10 Variation in sediment and velocity distribution in Pelton injector with needle angle

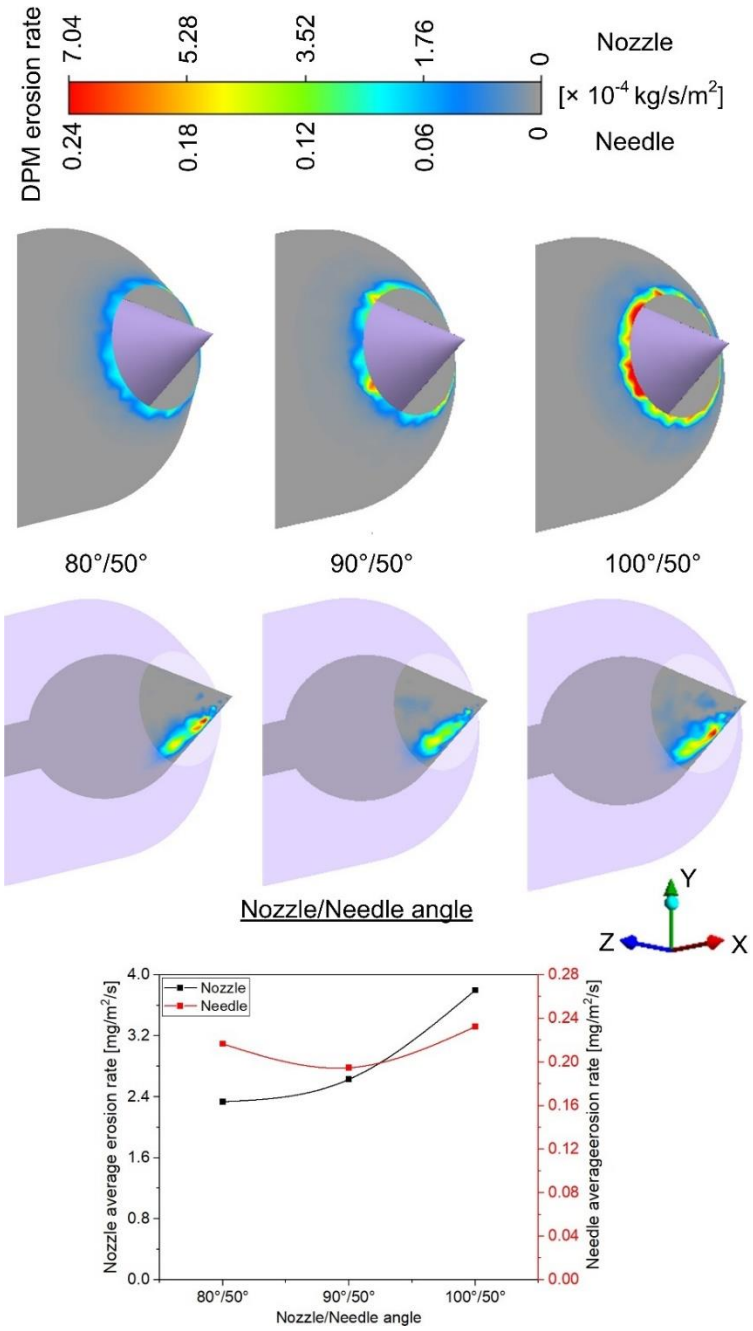

Fig. 11 Variation of erosion rate of nozzle and needle with nozzle angle

diminishes with the increase in needle angle as shown in Fig. 9. This is because needle with 40° tip angle is having more streamlined shape allowing sediment particles to more closely follow the fluid path. Hence, for a needle with a 40° tip angle sediment strikes both the upper and lower region of the needle but for the 60° case sediment strikes only in the lower region and not in the upper region of the needle as shown in Fig. 10.

3.3 Effect of Nozzle Angle

Variation in nozzle angle for a fixed needle angle affects the erosion process of both the nozzle and needle. On increasing the nozzle angle from 80° to 100°, an increase in the erosion rate of the nozzle is observed as shown in Fig. 11. This is due to the impingement of sediment particles at higher angles for nozzle with higher convergent angle. In the needle, the erosion rate decreases with an increase in nozzle angle from 80° to 90° as shown in Fig. 11. This is because as the nozzle angle increases from 80° to 90° convergent region increases, reducing the flow velocity for maintaining the continuity. As a result, the impact velocity of sediment particles striking the needle surface reduces, decreasing the erosion rate. However, with a further increase in nozzle angle from 90° to 100°, the erosion rate in the needle increases as shown in Fig. 11. This is due to an increase in the number of sediment particles reflecting from the nozzle at higher angles and striking the needle surface overtaking the effect of impingement of sediment particles with less velocity. Moreover, due to this same reason, erosion in the upper region of the needle can also be observed for a higher nozzle angle as shown in Fig. 11.

The variation of injector design does not merely govern the hydro-abrasive erosion but also the Pelton turbine efficiency. The variations in nozzle/needle angles

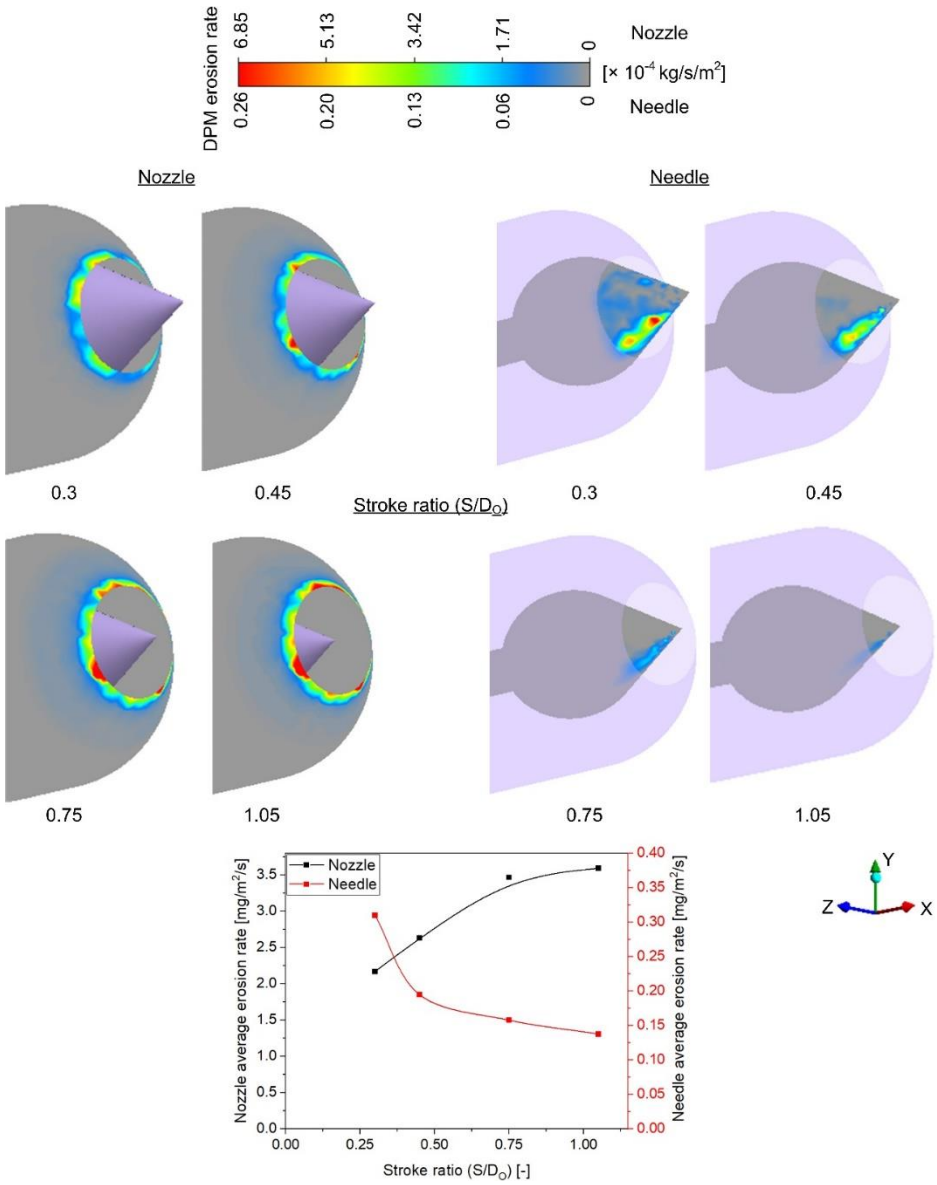

Fig. 12 Variation of erosion rate of nozzle and needle with stroke ratio

cause changes in the mass flow rate and jet quality, finally affecting the turbine efficiency (Benzon et al., 2015; Petley et al., 2019). Benzon et al. (2015) observed 0.5% increase in runner efficiency for a 110°/70° nozzle/needle angle design compared with a 90°/50° nozzle/needle angle combination. Therefore, for selecting the optimal design of Pelton injector, both hydro-abrasive erosion and turbine efficiency aspects need to be considered in erosion prone conditions.

3.4 Effect of Stroke Ratio

Other than the design of a Pelton injector, the operating condition also affects the erosion process of the injector. Here one of the operating parameters i.e., stroke ratio which depicts the nozzle opening is discussed. With the increase in stroke ratio or nozzle opening, discharge of sediment-laden water increases causing a greater number of sediment particles to strike the injector surface but simultaneously due to an increase in the convergent region or proximity between nozzle and needle surface, flow velocity reduces. This causes sediment to strike the injector surface with less impact force. The former phenomenon increases the erosion rate whereas the latter phenomenon has the potential to decrease the erosion rate. Hence, the overall change in the erosion rate of the nozzle and needle due to variation in stroke ratio depends on the phenomenon that is more prevailing or dominating.

It is observed as the stroke ratio increases from 0.3 to 0.75 erosion in the nozzle increases sharply this is due to an increase in discharge. However, with a further increase in stroke ratio from 0.75 to 1.05 erosion rate increases but the change is minimal due to a decrease in flow velocity as shown in Fig. 12. Overall, in the nozzle, discharge of sediment plays a dominant role, affecting the erosion rate. Fig. 13 shows a higher concentration of sediment near the nozzle exit for a 1.05 stroke ratio compared with a 0.3 stroke ratio. For the needle, an abrupt drop-in erosion rate is observed with an increase in stroke ratio from 0.3 to 0.45 due to a reduction in the average flow velocity of the convergent region. However, with a further increase in the stroke ratio from 0.45 to 1.05, the rate in the decrease of erosion rate reduces due to an increase in discharge as shown in Fig. 12. Overall, in

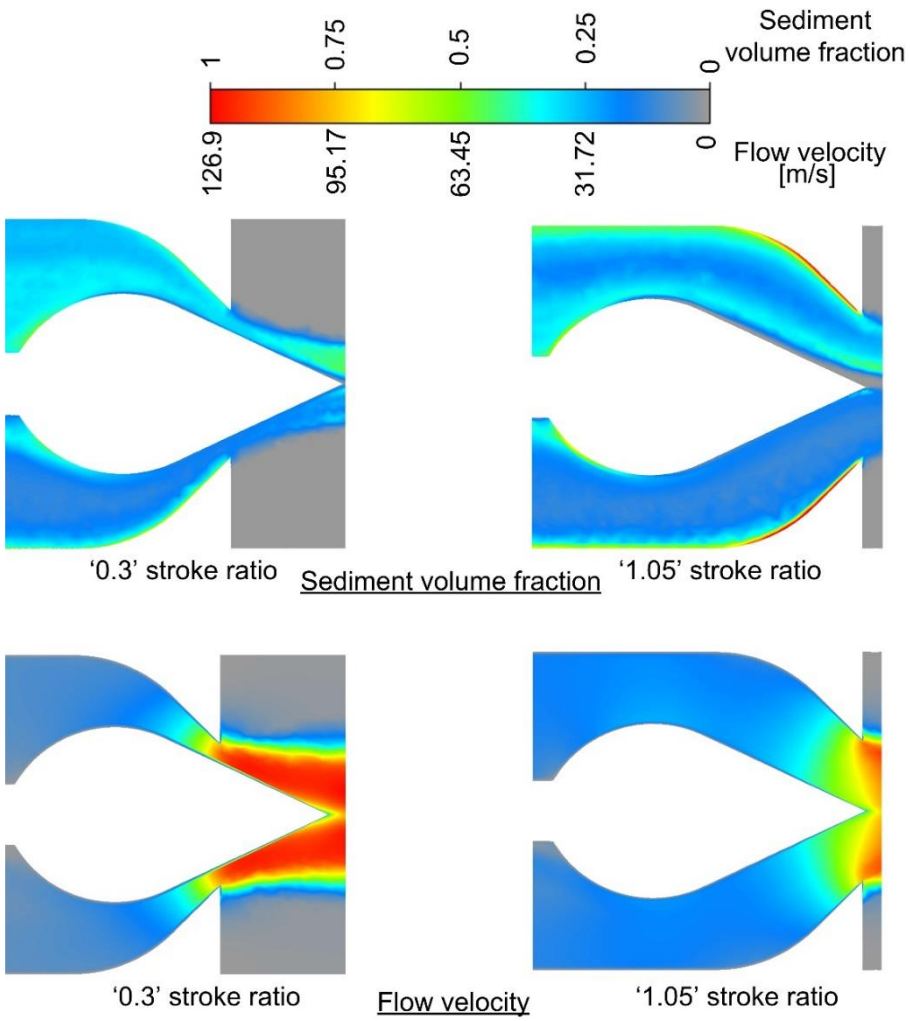

Fig. 13 Variation in sediment and velocity distribution in Pelton injector with stroke ratio

needle, flow velocity plays a dominating factor affecting the erosion rate. As shown in Fig. 13 more surface of the needle is exposed to a higher flow velocity region for 0.3 stroke ratio compared with the case of 1.05 stroke ratio. Moreover, the lesser the stroke ratio smaller will be the convergent region i.e., more proximity between the nozzle and needle surface allowing sediment to more closely follow the fluid path. As a result, for a 0.3 stroke ratio, erosion in the needle is also observed in the upper region along with the lower region whereas for a 1.05 stroke ratio proximity between the nozzle and needle surface reduces allowing sediment to detach from the upper region of the needle and hence erosion is observed only in the lower region of the needle as shown in Fig. 12.

From the obtained results it can be inferred, for the hydropower plants handling larger sediment size ($d_{90} \geq$ 100 µm) like Toss HPP (Rai et al., 2017), Chilime HPP (Bajrachrya et al., 2008) and Chenani HPP (Din & Harmain, 2020), erosion can be mitigated by optimizing the design parameters. For such HPPs, a bend angle below 90° should be considered while designing an injector. This is to avoid severe erosion in the nozzle and needle obtained beyond this angle as shown in Fig. 8. Further, 90°/50° will be the most optimum pair of nozzle/needle angle with respect to erosion. This is because at a needle angle, higher or lower than 50°, erosion in either of nozzle or needle increases considerably as shown in Fig. 9. Moreover, either increasing or decreasing the nozzle angle from 90° results in an increase of needle erosion as shown in Fig. 11. Whereas, for the hydropower plant like Chivor HPP (Morales, 2017) with d_{90} of 13.38 µm, the sediment particles will follow the fluid path more closely therefore variation of design parameter will not be much effective. In such a case along with the situation in which the design parameter of the powerplant is already fixed, optimizing the operating parameter will be beneficial in mitigating the erosion. From the obtained result, an injector operating at a stroke ratio of '0.45' is found to be most suitable. Since at higher and lower stroke ratios, erosion increases significantly in the nozzle and needle, respectively as shown in Fig. 12.

3.5 Effect of Needle Guide Vanes and Its Orientation

The pattern and intensity of erosion in a Pelton injector depends on the presence of needle guide vane (NGV) and its orientation. To analyze the influence of NGV, a needle guide with two vanes was considered in the injector geometry. In presence of NGV, the erosion of nozzle was merely impacted; whereas, a significant impact was observed in the erosion of the needle as shown in Fig. 14. The presence of NGV at 0° orientation has negligible impact on the erosion pattern of injector as compared with the erosion case of NGV-less configuration. As the presence of NGV influences the Dean vortices in 45° and 90° orientations by making the flow streamlined, the

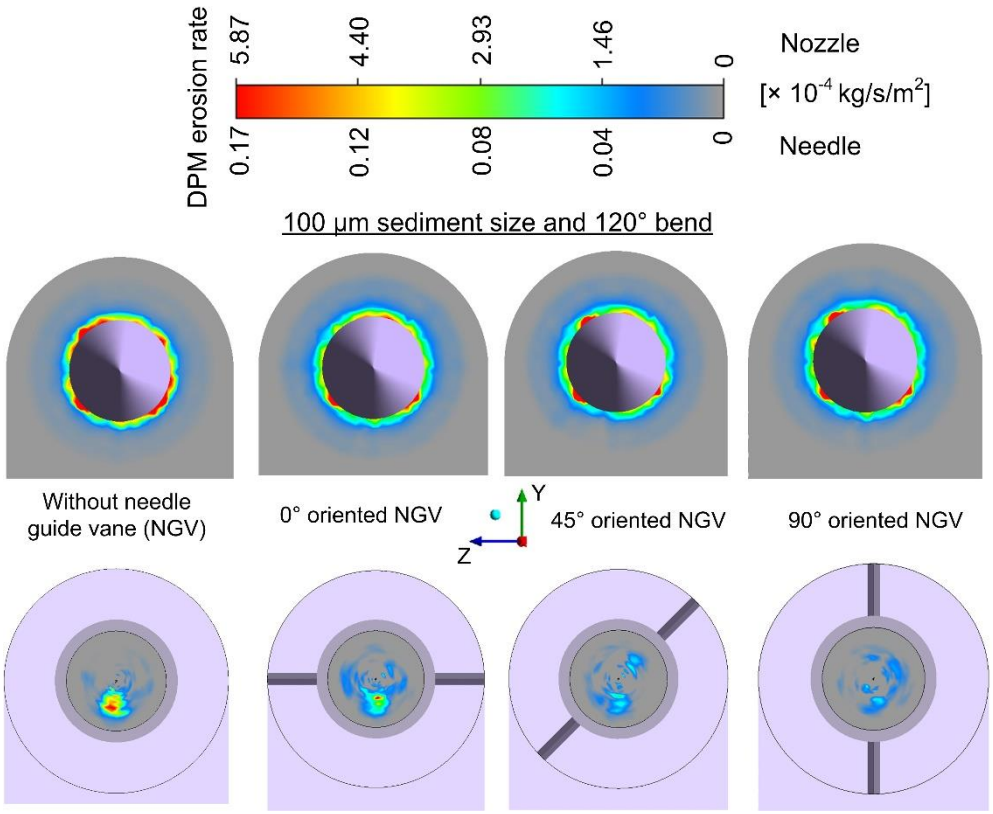

Fig. 14 Variation in erosion of Pelton injector with orientation of needle guide vane (NGV)

asymmetricity in erosion patterns reduces progressively. If bluff or less aerodynamically shaped NGV were used, then von-Karman vortices will predominate and affect the erosion pattern of needle as observed by Guo et al. (2020) while considering the straight nozzle pipe. Hence, an overall erosion in needle depends on the Dean vortices as well as von-Karman vortices. Therefore, to observe the sole effect of Dean vortices formed due to bend nozzle pipe on erosion, needle guide was not modelled while investigating the effect of design and operating parameters. Moreover, a 0° orientation of NGV has similar effects as the case of an NGV-less design as shown in Fig. 14.

4. CONCLUSION

The effect of design and operating parameters on the rate and pattern of hydro-abrasive erosion of the Pelton injector is discussed in this paper. The following list summarizes the key findings of this numerical study.

- Dean Vortices formation is observed in a Pelton injector having a bend and these Dean vortices are located towards the bend side. With the increase in the bend angle of the nozzle pipe, the size of the vortices increases simultaneously. As the flow velocity in near vortices is low compared to the other side of the bend sediment particles follows the fluid path more closely towards the bend side of the injector and this phenomenon is more predominant for higher bend angle.
- The effect of sediment size on the erosion process is observed differently for the nozzle and needle. Larger sediment causes more damage to the nozzle whereas the damage to the needle is more for smaller particle size. Further, irrespective of bend angle, asymmetricity in the erosion pattern of the needle is more profound for larger-size sediment particles.
- Variation in rate of erosion with bend angle is more extensive for larger-size sediment particles. Further, for larger sediment sizes, the susceptibility of the injector towards erosion increases with an increase in bend angle.
- A higher needle tip angle causes more erosion to the nozzle whereas a needle is more vulnerable to erosion for a lower needle angle. Moreover, asymmetricity in the erosion pattern of the needle increases with an increase in needle angle. Further, it is observed beyond 90° of the nozzle angles, the injector is at risk of damage as erosion of both the nozzle and needle increases.
- With the increase in stroke ratio, the rate of erosion in the nozzle increases whereas the needle is more susceptible to erosion for part-load condition. Further, asymmetricity in the erosion pattern of the needle increases with an increase in stroke ratio.

This study considered the case of a bend in different configurations in a simplified manner. In case a turbine typically has a distributor leading to the injectors, the flow is already distorted by the upstream bifurcations. As the complete distributor was not considered as a computational domain for analyzing the variation of design and operating parameters, the present study is limited in application to simplified cases only. To obtain

the erosion behavior of such injectors referring to this study, the flow pattern after the bifurcation in distributor is required to be used as inlet velocity condition.

ACKNOWLEDGEMENTS

The authors would like to thank Science and Engineering Research Board (Grant No. SRG/2020/002452), India for financially supporting the present work. The authors would also like to thank the Ministry of Education (MoE), Government of India for their financial help in the form of a Ph.D. scholarship.

CONFLICT OF INTEREST

The authors declare that they have no known competing financial interests or personal relationships that could have appeared to influence the work reported in this paper.

AUTHORS CONTRIBUTION

Conceptualization, investigation, methodology, writing - original draft was done by **Navam Shrivastava** and writing - review & editing, supervision was done by **Dr. Anant Kumar Rai**.

REFERENCES

Ansys Fluent Theory Guide 15.0 (2013).

Arora, N., Kumar, A., & Singal, S. K. (2022). Technological advancement in measurements of suspended sediment and hydraulic turbine erosion. *Measurement*, *190*, 110700. https://doi.org/10.1016/j.measurement.2022.110700

Bajracharya, T. R., Acharya, B., Joshi, C. B., Saini, R. P., & Dahlhaug, O. G. (2008). Sand erosion of Pelton turbine nozzles and buckets: A case study of Chilime Hydropower Plant. *Wear*, *264*(3-4), 177-184. https://doi.org/10.1016/j.wear.2007.02.021.

Bajracharya, T. R., Shrestha, R., & Timilsina, A. B. (2021). Numerical modelling of the sand particle flow in pelton turbine injector. *Journal of Engineering Issues and Solutions*, *1*(1), 88-105. https://doi.org/10.3126/joeis.v1i1.36821.

Bajracharya, T. R., Shrestha, R., Sapkota, A., & Timilsina, A. B. (2022). Modelling of hydroabrasive erosion in pelton turbine injector. *International Journal of Rotating Machinery*, 2022. https://doi.org/10.1155/2022/9772362.

Benzon, D., Zidonis, A., Panagiotopoulos, A., Aggidis, G. A., Anagnostopoulos, J. S., Papantonis, D. E. (2015). Numerical investigation of the spear valve configuration on the performance of Pelton and Turgo turbine injectors and runners. *Journal of Fluids Engineering*, *137*(11), 111201. https://doi.org/10.1115/1.4030628.

de Miranda, R. B., & Mauad, F. F. (2015). Influence of sedimentation on hydroelectric power generation: Case study of a Brazilian reservoir. *Journal of Energy Engineering*, *141*(3), 04014016. https://doi.org/10.1061/(ASCE)EY.1943-7897.0000183

Dedkov, A. P., & Gusarov, A. V. (2006). Suspended sediment yield from continents into the World Ocean: spatial and temporal changeability. *Sediment Dynamics and the Morphology of Fluvial Systems*, *306*, 3-11. https://dspace.kpfu.ru/xmlui/handle/net/140356.

Din, M. Z. U., & Harmain, G. A. (2020). Assessment of erosive wear of Pelton turbine injector: Nozzle and spear combination–A study of Chenani hydro-power plant. *Engineering Failure Analysis*, *116*, 104695. https://doi.org/10.1016/j.engfailanal.2020.104695.

Felix, D. (2017). Experimental investigation on suspended sediment, hydro-abrasive erosion and efficiency reductions of coated Pelton turbines. *VAW-Mitteilungen*, *238*. https://doi.org/10.3929/ethz-b-000161430

Forder, A., Thew, M., & Harrison, D. (1998). A numerical investigation of solid particle erosion experienced within oilfield control valves. *Wear*, 216(2), 184-193. https://doi.org/10.1016/S0043-1648(97)00217-2

Ge, X., Sun, J., Zhou, Y., Cai, J., Zhang, H., Zhang, L., & Zheng, Y. (2021). Experimental and numerical studies on opening and velocity influence on sediment erosion of Pelton turbine buckets. *Renewable Energy*, *173*, 1040-1056. https://doi.org/10.1016/j.renene.2021.04.072.

Guo, B., Xiao, Y., Rai, A. K., Zhang, J., & Liang, Q. (2020). Sediment-laden flow and erosion modeling in a Pelton turbine injector. *Renewable Energy*, *162*, 30-42. https://doi.org/10.1016/j.renene.2020.08.032.

Han, L., Zhang, G. F., Wang, Y., & Wei, X. Z. (2021). Investigation of erosion influence in distribution system and nozzle structure of Pelton turbine. *Renewable Energy*, *178*, 1119-1128. https://doi.org/10.1016/j.renene.2021.06.056.

Hirt, C. W., & Nichols, B. D. (1981). Volume of fluid (VOF) method for the dynamics of free boundaries. *Journal of Computational Physics*, *39*(1), 201-225. https://doi.org/10.1016/0021-9991(81)90145-5.

IEA. (2022). *World Energy Outlook*, IEA- International Energy Agency, Paris. https://www.iea.org/reports/world-energy-outlook-2022.

IEC 62364. (2019). *Guide for dealing with hydro-abrasive erosion in Kaplan, Francis, and Pelton turbines. Edition 2.0*. International Electrotechnical Commission. https://webstore.iec.ch/publication/27320

Jung, I. H., Kim, Y. S., Shin, D. H., Chung, J. T., & Shin, Y. (2019). Influence of spear needle eccentricity on jet quality in micro Pelton turbine for power generation. *Energy*, *175*, 58-65. https://doi.org/10.1016/j.energy.2019.03.077.

Koirala, R., Thapa, B., Neopane, H. P., Zhu, B., & Chhetry, B. (2016). Sediment erosion in guide vanes

of Francis turbine: A case study of Kaligandaki Hydropower Plant, Nepal. *Wear*, *362*, 53-60. https://doi.org/10.1016/j.wear.2016.05.013.

Liu, J., Yu, J., & Jiang, C. (2019, March). *Evaluation on sediment erosion of Pelton turbine flow passage component.* IOP Conference Series: Earth and Environmental Science. IOP Publishing. https://doi.org/10.1088/1755-1315/240/2/022027.

Luis, J., Sidek, L. M., & Jajarmizadeh, M. (2016, March). *Impact of sedimentation hazard at Jor Reservoir, Batang Padang hydroelectric scheme in Malaysia.* IOP Conference Series: Earth and Environmental Science. IOP Publishing. https://doi.org/10.1088/1755-1315/32/1/012030.

Messa, G. V., Mandelli, S., & Malavasi, S. (2019). Hydro-abrasive erosion in Pelton turbine injectors: A numerical study. *Renewable Energy*, *130*, 474-488. https://doi.org/10.1016/j.renene.2018.06.064.

Morales, A. M. B., Pachón, I. F., Loboguerrero, J., & Medina, J. A. (2017). Development of a test rig to evaluate abrasive wear on Pelton turbine nozzles. A case study of Chivor Hydropower. *Wear*, *372*, 208-15. https://doi.org/10.1016/j.wear.2016.11.003.

Oka, Y. I., & Yoshida, T. (2005). Practical estimation of erosion damage caused by solid particle impact: Part 2: Mechanical properties of materials directly associated with erosion damage. *Wear*, *259*(1-6), 102-109. https://doi.org/10.1016/j.wear.2005.01.040

Oka, Y. I., Okamura, K., & Yoshida, T. (2005). Practical estimation of erosion damage caused by solid particle impact: Part 1: Effects of impact parameters on a predictive equation. *Wear*, *259*(1-6), 95-101. https://doi.org/10.1016/j.wear.2005.01.039

Padhy, M. K., & Saini, R. P. (2008). A review on silt erosion in hydro turbines. *Renewable and Sustainable Energy Reviews*, *12*(7), 1974-1987. https://doi.org/10.1016/j.rser.2007.01.025.

Padhy, M. K., & Saini, R. P. (2009). Effect of size and concentration of silt particles on erosion of Pelton turbine buckets. *Energy*, *34(*10), 1477-1483. https://doi.org/10.1016/j.energy.2009.06.015.

Padhy, M. K., & Saini, R. P. (2011). Study of silt erosion on performance of a Pelton turbine. *Energy*, *36*(1), 141-147. https://doi.org/10.1016/j.energy.2010.10.060.

Padhy, M. K., & Saini, R. P. (2012). Study of silt erosion mechanism in Pelton turbine buckets. *Energy*, *39*(1), 286-293. https://doi.org/10.1016/j.energy.2012.01.015.

Petley, S., Zidonis, A., Panagiotopoulos, A., Benzon, D., Aggidis, G. A., Anagnostopoulos, J. S., & Papantonis, D. E. (2019). Out with the old, in with the new: Pelton hydro turbine performance influence utilizing three different injector geometries. *Journal of Fluids Engineering*, *141*(8), 081103. https://doi.org/10.1115/1.4042371.

Rai, A. K., & Kumar, A. (2015). Continuous measurement of suspended sediment concentration: Technological advancement and future outlook, *Measurement*, *76*, 209-227. https://doi.org/10.1016/j.measurement.2015.08.013.

Rai, A. K., Kumar, A., & Staubli, T. (2017). Hydro-abrasive erosion in Pelton buckets: Classification and field study, *Wear*, *392*, 8-20. https://doi.org/10.1016/j.wear.2017.08.016

Rai, A. K., Kumar, A., & Staubli, T. (2019). Analytical modelling and mechanism of hydro-abrasive erosion in Pelton buckets, *Wear*, *436-437*, 203003. https://doi.org/10.1016/j.wear.2019.203003.

Rai, A. K., Kumar, A., & Staubli, T. (2020). Effect of concentration and size of sediments on hydro-abrasive erosion of Pelton turbine, *Renewable Energy*, *145*, 893-902. https://doi.org/10.1016/j.renene.2019.06.012.

Rai, A. K., Kumar, A., Hies, T., & Nguyen, H. H. (2016, November). *Field application of a multi-frequency acoustic instrument to monitor sediment for silt erosion study in Pelton turbine in Himalayan region, India.* IOP Conference Series: Earth and Environmental Science. IOP Publishing. https://doi.org/10.1088/1755-1315/49/12/122004.

Sangal, S., Singhal, M. K., & Saini, R. P. (2018). Hydro-abrasive erosion in hydro turbines: a review. *International Journal of Green Energy*, *15*(4), 232-253. https://doi.org/10.1080/15435075.2018.1431546.

Shrivastava, N., & Rai, A. K. (2023). *Assessment of sediment hazard and associated measurement*. River Dynamics and Flood Hazards: Studies on Risk and Mitigation. Singapore: Springer Nature Singapore. https://doi.org/10.1007/978-981-19-7100-6_2.

Singh, J., & Nath, S. K. (2022). Surface and bulk modification techniques to mitigate silt erosion in hydro turbines: a review of techniques and parameters. *Surface Engineering*, *38*(3), 288-302. https://doi.org/10.1080/02670844.2022.2082750.

Staubli, T., Abgottspon, A., Weibel, P., Bissel, C., Parkinson, E., Leduc, J., & Leboeuf, F. (2009a). Jet quality and Pelton efficiency. *Proceeding of Hydro-2009, Lyon, France*. https://www.researchgate.net/publication/290989838_Jet_quality_and_Pelton_efficiency

Staubli, T., Abgottspon, A., Weibel, P., Bissel, C., Parkinson, E., & Leduc, J. (2009b). Die auswirkung der strahlqualität auf den wirkungsgrad von peltonturbinen. *Wasser Energ. Luft*, *101*(3), 181-188. https://www.researchgate.net/publication/290989575_Die_Auswirkung_der_Strahlqualitat_auf_den_Wirkungsgrad_von_Peltonturbinen

Staubli, T., Weibel, P., Bissel, C., Karakolcu, A., & Bleiker, U. (2010, November). *Efficiency increase by jet quality improvement and reduction of splashing water in the casing of Pelton turbines.* 16th International Seminar on Hydropower Plants. https://www.researchgate.net/publication/228496314_Efficiency_increase_by_jet_quality_improvement_and_reduction_of_splashing_water_in_the_casing_of_Pelton_turbine

Tarodiya, R., Khullar, S., & Levy, A. (2022). Assessment of erosive wear performance of Pelton turbine injectors using CFD-DEM simulations. *Powder Technology*, *408*, 117763. https://doi.org/10.1016/j.powtec.2022.117763.

Thapa, B. S., Dahlhaug, O. G., & Thapa, B. (2015). Sediment erosion in hydro turbines and its effect on the flow around guide vanes of Francis turbine. *Renewable and Sustainable Energy Reviews*, *49*, 1100-1113. https://doi.org/10.1016/j.rser.2015.04.178.

Xu, L., Zhang, Q., Zheng, J., & Zhao, Y. (2016). Numerical prediction of erosion in elbow based on CFD-DEM simulation. *Powder Technology*, *302*, 236-246. https://doi.org/10.1016/j.powtec.2016.08.050.

Zhang, Z. (2016). Injector Characteristics. *Pelton Turbines*, 29-51. https://doi.org/10.1007/978-3-319-31909-4_3

Zhang, Z., & Casey, M. (2007). Experimental studies of the jet of a Pelton turbine. *Proceedings of the Institution of Mechanical Engineers, Part A: Journal of Power and Energy*, *221*(8), 1181-1192. https://doi.org/10.1243%2F09576509JPE408